Available online at www.sciencedirect.com
SCIENCE DIRECT®
Journal of Hydrology 281 (2003) 206–229
Journal of Hydrology
www.elsevier.com/locate/jhydrol

Towards estimation of extreme floods: examination of the roles of runoff process changes and floodplain flows

Chatchai Jothityangkoon, Murugesu Sivapalan*

Centre for Water Research, Department of Environmental Engineering, The University of Western Australia, 35 Stirling Highway, Crawley, WA 6009, Australia

Received 30 May 2002; accepted 23 June 2003

Abstract

This paper presents the development and application of a distributed rainfall–runoff model for extreme flood estimation, and its use to investigate potential changes in runoff processes, including changes to the 'rating curve' due to effects of over-bank flows, during the transition from 'normal' floods to 'extreme' floods. The model has two components: a hillslope runoff generation model based on a configuration of soil moisture stores in parallel and series, and a distributed flood routing model based on non-linear storage–discharge relationships for individual river reaches that includes the effects of floodplain geometries and roughnesses. The hillslope water balance model contains a number of parameters, which are measured or derived a priori from climate, soil and vegetation data or streamflow recession analyses. For reliable estimation of extreme discharges that may extend beyond recorded data, the parameters of the flood routing model are estimated from hydraulic properties, topographic data and vegetation cover of compound channels (main channel and floodplains). This includes the effects of the interactions between the main channel and floodplain sections, which tend to cause a change to the rating curve. The model is applied to the Collie River Basin, 2545 km^2, in Western Australia and used to estimate the probable maximum flood (PMF) from probable maximum precipitation estimates for this region. When moving from normal floods to the PMFs, application of the model demonstrates that the runoff generation process changes with a substantial increase of saturation excess overland flow through the expansion of saturated areas, and the dominant runoff process in the stream channel changes from in-bank to over-bank flows. The effects of floodplain inundation and floodplain vegetation can significantly reduce the magnitude of the estimated PMFs. This study has highlighted the need for the estimation of a number of critical parameters (e.g. cross-sectional geometry, floodplain vegetation, soil depths) through concerted field measurements or surveys, and targeted laboratory experiments.

Keywords: Extreme floods; Process changes; Rating curve; Rainfall–runoff model; Floodplains; Compound channels; Probable maximum flood

1. Introduction

The focus of this paper is on extreme floods, and the fundamental problems associated with their estimation, illustrating these through the particular example of an application in Western Australia.

* Corresponding author. Tel.: +61-8-9380-2320; fax: +61-8-9380-1015.
E-mail address: sivapalan@cwr.uwa.edu.au (M. Sivapalan).

0022-1694/03/$ - see front matter © 2003 Elsevier B.V. All rights reserved.
doi:10.1016/S0022-1694(03)00237-3

The models presented are specific to this region, yet the issues covered by this paper are universal and address difficulties faced by engineering hydrologists worldwide. By way of clarification, the extreme flood we are interested in here is the so-called probable maximum flood (PMF). The PMF is a river discharge with a very small exceedance probability, and is the design standard for the design of hydraulic structures whose failure could lead to catastrophic loss of life. Typically, in engineering practice, the PMF is estimated by transforming the probable maximum precipitation (PMP), similarly defined as the maximum possible rainfall event for the location and time period of interest. The transformation from PMP to PMF is achieved by using appropriate hydrologic methods. Note that despite the word 'probable' in their names, a realistic exceedance probability or return period cannot be assigned to either the PMP or PMF. Even if assigned, the return period will be necessarily large, perhaps of the order of tens of thousands of years or more (Klemes, 1993; Foufoula-Georgiou, 1989; Pilgrim and Rowbottom, 1987), and therefore cannot be verified in practice.

Two main hydrologic methods are currently in use for transforming PMPs to PMFs: the use of continuous simulation models and the unit hydrograph method (Pilgrim and Rowbottom, 1987). This study is focused on the use of continuous simulation approach, which has a number of advantages over the unit hydrograph method: (i) the ability to incorporate complex physical processes contributing to catchment runoff responses, and their inherent non-linearities; (ii) the potential to take into account the spatial variability of catchment properties and rainfall–runoff processes; (iii) the ability to incorporate natural or human induced changes to catchment characteristics.

Examples of hydrological models used for extreme flood estimation in Australia are the RORB runoff routing model of Laurenson and Mein (1988), the watershed bounded network model (WBNM) of Boyd et al. (1979), and the piecewise linear (PLM) and the quasi-linear (QLM) models of Bates and Pilgrim (1986). However, the models mentioned above are mainly runoff routing models, and similar to unit hydrograph methods they require, prior to the routing, a loss model which is able to convert the rainfall hyetograph to a rainfall excess hyetograph. The recommended practice in Australia is to use regionalised methods, which are often based on previous engineering practice and experience. For example, in the south-west of Western Australia, Australian Rainfall and Runoff (Pilgrim and Rowbottom, 1987) recommends the use of the so-called initial loss-continuing loss method using specified parameter values. The recommended method and the parameter values specified are, however, not based on a true appreciation of the processes that may lead to flooding in the region, and many hydrologists feel that these methods may give rise to overestimates. Thus, an investigation of the potential mechanisms that cause extreme floods in this region would be valuable to give more insights into appropriate methods of extreme flood estimation. This is the motivation for the work that is presented in this paper.

The application of continuous simulation models for extreme flood estimation suffers from the drawback that most models rely on calibration for the estimation of their parameter values. It goes without saying that such calibrations will be carried out using observed, less-than-extreme floods, and the extrapolation to extreme floods will not be able to explicitly consider that observed flood events and extreme flood events may well be dominated by different rainfall–runoff processes. Thus, an appreciation of likely change of processes that may occur when we go from 'normal' to extreme floods is an important consideration, and where possible these have to be factored in extreme flood estimation.

The phenomenon of change of process with increasing return period is well understood in hydrology (Sivapalan et al., 1990; Wood et al., 1990). The dominant process of runoff generation can change with the increase of storm event size (depth), and this change of process with increasing return period may be reflected in the shape of flood frequency curve. For example, using the derived flood frequency method involving a non-linear rainfall–runoff model, Sivapalan et al. (1990) showed for hypothetical catchments that the dominant runoff generation process can change from saturation excess overland flow to infiltration excess overland flow with increasing return period.

In stream channels, a similar change of channel flow processes can be observed, both in actual rivers and laboratory experiments. In this case, over-bank flow takes over from in-bank flow when the inputs to

the river, either from an upstream reach of the river or from the adjacent catchment area, exceed the capacity of the main channel to carry this flow. A number of laboratory experiments have been carried out to investigate the effects of compound channels, including the mass and momentum transfer between the main channel and floodplain (Wormleaton and Merrett, 1990). Wormleaton and Merrett, using a laboratory flume with a compound trapezoidal cross-section, investigated the effects of different channel geometries and roughnesses, by varying the ratio of floodplain width to the main channel width, and the Manning coefficient associated with floodplain roughness. They found that the stage–discharge curves (i.e. the rating curves) of the over-bank and in-bank flows were different. Similar conclusions were drawn about the effects of floodplain inundation by Bates and Pilgrim (1983) and Kölla (1987). Recently, Woltemade and Potter (1994) examined flood peak attenuation under many geomorphic conditions using the MIKE 11 rainfall–runoff and hydrodynamic models. They showed that channel-terrace morphology, valley width, stream slope and hydraulic roughness influence peak discharges, especially for moderate flood magnitudes (5–50 years return periods).

Despite these observations, the effects of change of processes, such as the expansion of saturated areas on hillslopes and floodplain inundation, fail to be recognised explicitly in the estimation of extreme floods. The objective of this paper is to present an extreme flood estimation model that uses an existing long-term water balance model, presented in Jothityangkoon et al. (2001), combined with a routing scheme that uses an extension of the observed rating curve to incorporate the effects of floodplain vegetation and topography. The runoff generation component of this new extreme flood model utilises field-measured information on the distribution of soil depths, while its runoff routing component is based on explicit treatment of both floodplain storage and the resistance to flow due to floodplain vegetation. In particular, the model can account for the change of processes with respect to both the runoff generation and runoff routing processes. This new modelling approach is applied to the Collie River Basin in south-west Western Australia, for which all of the model parameters can in principle be estimated a priori without calibration. We use this model to also explore likely changes to runoff processes in this catchment as we move from normal floods to extreme floods. We use the results to make inferences about the types of process models that should be used to estimate extreme floods, and about the types of additional information that need to be assembled for a more reliable estimation of extreme floods in this region.

This paper begins with a brief description of the model previously used in this catchment for extreme flood estimation. This is followed by a summary of the model generalisations that we have adopted in this paper to explicitly account for processes that are likely to operate under extreme flood conditions in this catchment. In Section 3, we present details of the proposed model components for runoff generation and runoff routing. Application to Collie River Basin is presented in Section 4, including parameter estimation, model validation, and PMP estimation. The final section presents the application of the model for extreme flood estimation, and a comparison with PMF estimates produced by previous approaches. We also use the model results to explore process changes that are likely to occur in this catchment in the transition from normal to extreme floods.

2. Approaches to extreme flood modelling

2.1. Models used currently in Western Australia (based on RORB)

This section begins with a brief description of models currently used in Australia for the estimation of extreme floods. These generally contain two major components (Fig. 1(a)): (i) a rainfall loss model—this can be a constant loss rate or runoff coefficient applied to the PMP, or a model based on an initial loss followed by a continuing constant or variable loss rate; (ii) a distributed runoff routing model over the river network, conceptualised as a series of non-linear reservoirs. The RORB model (Laurenson and Mein, 1988) is the standard model often used, and it has built in standard features and recommended practices for both of these two elements.

However, hydrologists in Western Australia have found that loss models hardwired into RORB

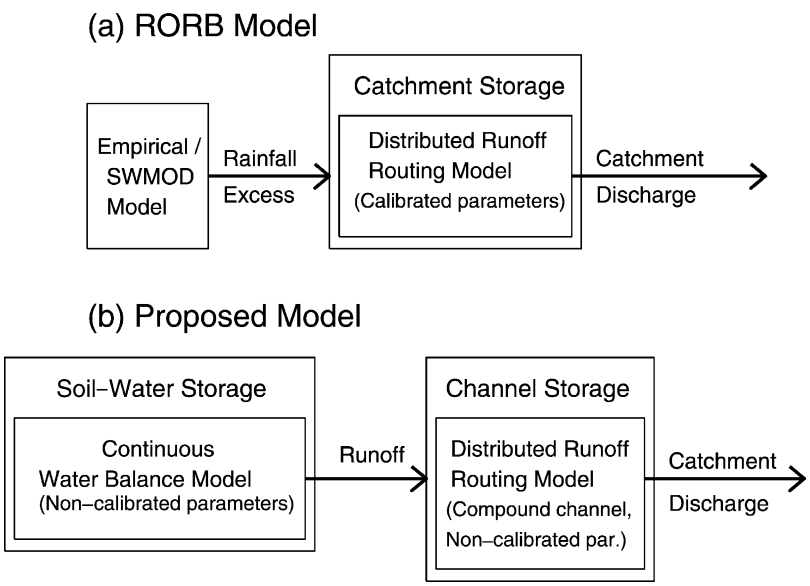

Fig. 1. Schematic of the RORB model and the distributed rainfall–runoff model used in this study.

(e.g. initial loss-continuing loss model) are inadequate for the catchments in the south-west region of Western Australia, with deep permeable soils. Stokes (1989) has suggested, for PMF estimation purposes only, a loss model based on measured distribution of soil depths and assumed porosity values. This variable bucket capacity model, called SWMOD, generates saturation (storage) excess runoff when the soil profiles are saturated with water, and has the built in potential to generate partial area runoff generation. However, it is very simple and does not include subsurface stormflow, which is the dominant mechanism of runoff generation in this region, and so the model cannot be applied to predict normal or observed flood events.

A rainfall loss model, such as SWMOD, estimates the rate of runoff generation (rainfall excess hyetograph) during the event. This becomes the input to the routing model, which transports this water down the channel network, and produces the discharge hydrograph at the catchment outlet. The PMF is then the peak of the resulting hydrograph. A non-linear storage–discharge relationship, given by $S = kQ^m$, which is the basis of runoff routing in each link of the stream network, represents in a lumped manner all of the hydraulic processes governing flow in a river reach. The parameters, k and m, as in traditional flood routing methods, are estimated by calibration with respect to observed, representative flood events. There is allowance for k and m to be spatially variable across the network.

Investigation of the sources of non-linearity described above has focussed more on the routing process rather than on the runoff generation processes, even though the latter could well be strongly non-linear. Wong (1989) applied the RORB model to three eastern Australian catchments, and found evidence to suggest that the form of the storage–discharge relationship consists of two primary non-linear power functions, one for in-bank flows and another for over-bank flows. However, a priori estimation of these functions, applicable to PMF estimation, remains a problem.

2.2. Proposed extreme flood model framework

The model framework proposed in this paper (Fig. 1(b)) is a considerable advance over the previous model in a number of different ways. Firstly, the loss model is replaced by a continuous hillslope water balance model which (a) includes runoff generation by saturation (storage) excess as well as subsurface

storm flow, and (b) can be applied to catchments in south-west Western Australia with no or minimal calibration on observed flood events. This means that the model can be used to simulate normal or observed flood events. Secondly, because the parameters are estimated a priori based on field data on soils, including the same soil depth information that goes into SWMOD, it can be used with confidence for extreme flood events. Furthermore, since it is a continuous water balance model, the effects of antecedent soil wetness can be simulated quite easily. The model is operated on a daily time step for long-term water balance calculations, and to set the right antecedent soil moisture conditions, and is then operated on an hourly time step for event simulations.

The runoff routing component of the proposed model is very similar to the RORB model, in that it divides the catchment into a network of non-linear reservoirs, each of which represents an individual channel reach. The storage–discharge relationship is similarly expressed by $S = kQ^m$, as in RORB. However, there are two main differences to the previous model. Firstly, runoff contributions to the channels from catchment areas are generated by the hillslope water balance model described previously. Secondly, the parameters k and m are no longer estimated by calibration with observed, less-than-extreme flood events, but estimated a priori based on hydraulic characteristics of the main channel (often expressed through empirical stage–discharge curves) and of the floodplains and associated roughnesses. The features described above make it possible to use the proposed model to investigate possible change of processes in the transition from normal to extreme floods, which is an important objective of this paper.

3. Development and testing of extreme flood model components

3.1. Hillslope water balance model

The hillslope water balance model used here is an adaptation of a sub-catchment based, distributed water balance model developed by Jothityangkoon et al. (2001). This model divides a large catchment into a number of sub-catchments organised around its stream network. The model is conceptualised in terms of a distribution of 'buckets' of various sizes, arranged in series (to capture within sub-catchment variability of soil depths and hydraulic properties), and in parallel (to capture spatial variabilities of climate and soils between sub-catchments). The model includes saturation excess overland flow, subsurface stormflow, deeper groundwater flow, bare soil evaporation and plant transpiration. These are parameterised in terms of the level of soil water storage in these buckets. Due to the highly permeable topsoils in the region, often an order of magnitude larger than the highest observed rainfall intensities, infiltration excess runoff is almost non-existent in this region and is not included in the model. They have also been ignored in previous extreme flood estimation procedures (Stokes, 1989).

Parameters of the model are estimated a priori based on available data, and therefore the model does not rely on calibration for their estimation, which is an important qualification for models to be used in estimating extreme floods. In particular, the model utilised considerable information on distributions of soil depth that were available in this region. The model has been developed in progressive steps, at the annual, monthly and daily time scales, and its predictions have been tested against signatures of runoff variability at each scale. The model version with a daily time step has been constructed with the minimum complexity and parameters needed to capture daily runoff variability. More details of the model are given in Jothityangkoon et al. (2001).

For prediction of extreme flood events, the model with a daily time step may not be sufficient to obtain accurate estimates of the peak flows needed for design purposes. For this reason, additional work was done in this paper to convert it to an hourly model. The previous version of the model ignores the delay in the unsaturated zone, assuming all incoming rainfall to reach the saturated zone (perched water table) directly within the single time step. This may be satisfactory in a daily model, but clearly unrealistic when using an hourly time step. It therefore calls for a modification to introduce a delay mechanism in the unsaturated zone for hourly predictions.

The delay in the unsaturated zone is modelled simply by treating the unsaturated zone as a separate

soil moisture store, and by continuously monitoring its water balance. The unsaturated zone receives water from rainfall, and releases some of this water to the saturated zone below—this percolation is governed by the unsaturated hydraulic conductivity K_h of the soil, which is a function of the moisture content. The parameters of the delay process are the saturated hydraulic conductivity, the depth of soil, and soil parameters. The delay scheme is presented in summary form in Appendix A.

There are three attractions of the model we have presented above to the application considered here: (i) it is a continuous model, and can be used to predict the antecedent wetness (i.e. summer versus winter conditions) prior to the application of the PMP, (ii) it has all of the processes of runoff generation that are likely in this catchment, and hence it can handle any change of processes which is likely to occur under different weather conditions, as demonstrated by Jothityangkoon and Sivapalan (2001), and (iii) the parameters are estimated a priori based on field data, especially of soil depths, and not based on calibration, and hence the model can be used with confidence to extrapolate to extreme flood conditions.

3.2. Runoff routing model

The hillslope water balance model we presented above is based on the subdivision of the catchment into a number of sub-catchments organised around the channel network. This subdivision is necessary to include the effects of spatial variability of rainfall, soil and vegetation on runoff processes. Runoff from each sub-catchment, estimated by the hillslope water balance model described previously, is delivered to the associated stream channel, and routed down the channel network.

The routing model we use here is not based on the solution of traditional balance equations, i.e. St Venant equations, governing flow in rivers. Rather, the model is based on a conceptualisation of each channel link in the network as a non-linear reservoir. In many respects this is similar to the RORB model mentioned previously (Laurenson and Mein, 1988). The response of each channel reach is modelled by solving its water balance equation $dS/dt = I(t) - Q(t)$, combined with a non-linear storage (S) to discharge (Q) relationship which is given in the form of a power function of the form:

$$S = kQ^m \tag{1}$$

where k and m are model parameters, and $I(t)$ represents an input hydrograph, which is equal to the summation of inflows from the adjacent catchment area, and inflows at the upstream end of the reach in question from possibly two upstream reaches. The parameters k and m must be estimated for each of the stream reaches forming the network, and should accommodate the variation of these properties in the downstream direction with increase of catchment area, and associated deepening and widening of the river channels.

In order to give a physical meaning to the parameters k and m, we write down the relationship between storage and discharge using the average velocity across the channel cross-section. Noting that $Q = Av$, and $S = AL$, where A is the cross-sectional area, L is the length of the river reach, and v the velocity, this gives the following storage–discharge relationship:

$$S = LA = \frac{L}{v}Q \tag{2}$$

If v is a constant, irrespective of Q, then this gives rise to a linear storage–discharge relationship with $k = L/v$, and $m = 1$. If on the other hand, v varies with flow, then in general we obtain a non-linear relationship, and the k and m parameters depend on the variation of v with discharge. For example, assuming the Chezy equation to estimate velocity in a wide rectangular channel of width w and a Chezy coefficient C, Menabde and Sivapalan (2001) showed that:

$$k = C^{-2/3}S_0^{-1/3}w^{1/3}L \text{ and } m = 2/3 \tag{3a}$$

where S_0 is the channel slope. On the other hand, in terms of the Manning's coefficient, these are given by:

$$k = n^{3/5}S_0^{-3/10}w^{1/5}L \text{ and } m = 3/5 \tag{3b}$$

One finds that when the flow is confined within the main channel of a river (below bankfull discharge) the exponent obtained is roughly consistent with the Manning or Chezy formulation given above, and velocity increases with the flow. When bankfull discharge is exceeded, this gives rise to a retardation of the flow, and velocity tends to increase more

slowly, eventually remaining constant with further increases in discharge beyond a threshold (Bates and Pilgrim, 1983; Wong and Laurenson, 1983). This gives rise to a linear storage–discharge relationship eventually, as given by Eq. (2) above, with $m = 1$. Thus, over the full range of flows possible in a river, the exponent m in the storage–discharge relationship varies from about 0.6 to 1.0. In summary, the transition from normal floods to extreme floods is accompanied by substantial changes to the character of river flow, and to parameters k and m.

An example of the estimation of the parameters k and m in the transition from in-bank to over-bank flows is presented next based on laboratory experiments performed by Wormleaton and Merrett (1990), the experimental set-up of which is presented in Fig. 2(a). The experiments were performed for different compound channel geometries, and different

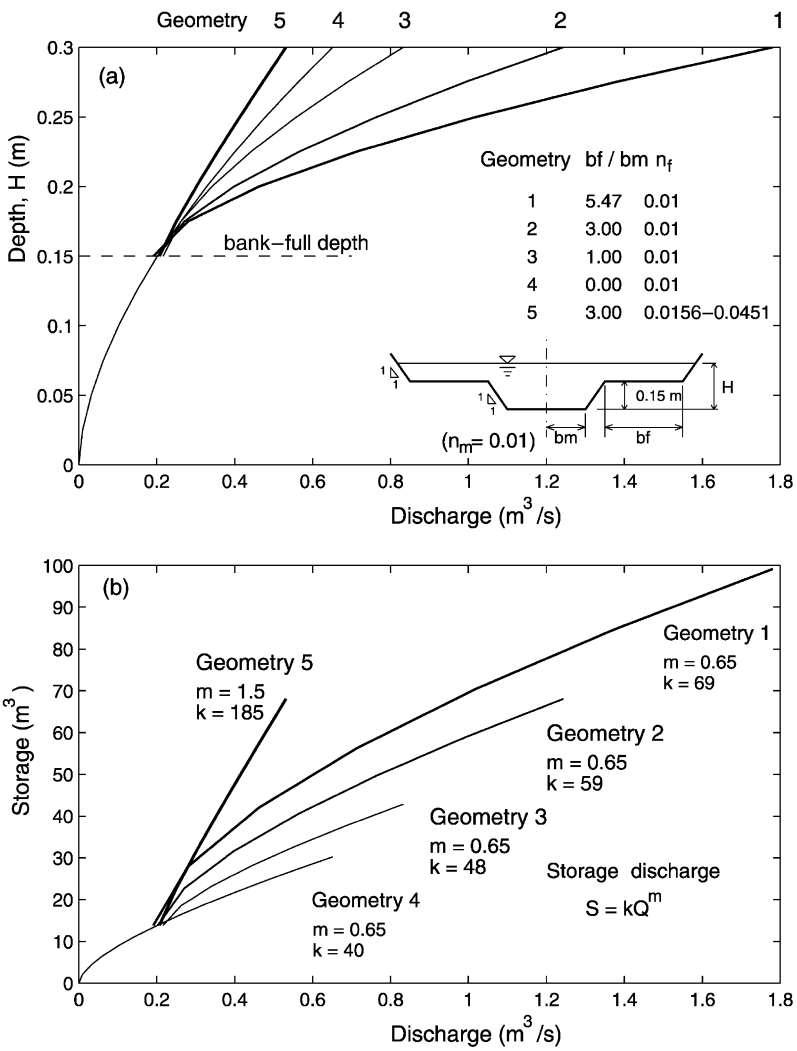

Fig. 2. Results from the hydraulic laboratory experiments carried out by Wormleaton and Merrett (1990), (a) stage–discharge curve for five geometries, (b) estimates storage–discharge curves and estimates of k and m for the five geometries. NB: n_m and n_f denote the Manning coefficients for the main channel and floodplain, respectively.

types of roughnesses in the main channel and floodplain. Fig. 2(a) also presents the relationship between stage, H, and measured discharge, Q, for these different configurations. In all experiments the Manning coefficient for the main channel, n_m, was kept the same at 0.01 while that of floodplain n_f was varied. We can note, firstly, that when $n_f = n_m$, an increase in the size of the floodplain leads to an increase in discharge but the rate of increase is, predictably, smaller. When $n_f > n_m$, the resulting total discharge is actually smaller than for $n_f = n_m$, but more interestingly, it is also smaller than that for the main channel operating alone. This suggests that, in this case, the effect of the floodplain is to retard the discharge that would otherwise have occurred in the main channel. This retardation must also be taken into account in estimating extreme floods, if found to be significant.

Fig. 2(a), in combination with the flow area versus height curves for the various channel cross-sections and the length of the flume, can be used to construct the corresponding storage–discharge curves. These are presented in Fig. 2(b). We find that the storage–discharge curve progressively undergoes a transformation from that of the main channel (geometry 4) to that of the floodplain, with the parameters k and m being dependent on the geometry as well as the relative roughness of the floodplain. When $n_f = n_m$ the final values of m for geometries 1–4 are the same, and k increases with increasing floodplain width. There is, however, a transition zone between the main channel and floodplain. For $n_f > n_m$, both m and k values are larger in the transition region between main channel and floodplain dominance.

3.3. Estimation of k and m for actual rivers for extreme flood estimation

Estimation of the parameters k and m is fairly straightforward when the flow is restricted to the main channel. In this case, the effect of flow resistance is easily captured by directly using recorded stage–discharge curves (known as rating curves), combined with available information on the flow area versus height relationship, estimated from the geometry of main channel cross-section, and the length of the river reach.

Many rating curves do contain information on over-bank flows, as streams typically go over-bank, on average, once in about 2–3 years. However, the rating curves may not include the effects of the extent of over-bank flows experienced during extreme floods similar in magnitude to PMFs. Quite often there is no recorded data under these conditions due to the rarity of these extreme events, and the difficulty in carrying out hydrographic measurements. Therefore, estimation of the rating curves beyond recorded data has to be accomplished by means of scaled laboratory experiments or detailed numerical models. In this paper, we use a somewhat simpler approach: we subdivide the compound channel into main channel and floodplain sections. Discharge in each section is estimated separately. In the case of the main channel, the empirical storage–discharge curve is used directly. In the case of the floodplain, an equivalent Chezy coefficient is estimated using a methodology developed by Tamai (1992a,b), based on explicit consideration of the effects of vegetation and other roughnesses that may be present in the floodplain. The two discharges are then combined together to estimate a total discharge, having explicit regard to possible retardation effects caused by floodplain flows on the flows in the main channel. Details of this procedure are described next.

3.3.1. Floodplain resistance

For the purpose of flood prediction in remote areas in north-west Western Australia, Tamai (1992a,b) proposed an analytical approach for the estimation of flow resistance due to turbulent over-bank flow, consisting of two parts: surface (frictional) resistance and form drag. In the presence of tall vegetation in floodplains, the form drag arises due to two factors: (i) flow past immersed bodies such as tree trunks, and (ii) drag arising from energy dissipation by coherent eddy patches formed around the leaves of bushes or trees. Apart from the form drag, resistance from bare soil or short vegetation patches, such as grasses, is considered similarly for the main channel and floodplain. A conventional resistance formula such as the Chezy or Manning equation, is used to estimate the resistance due to this surface drag. Given the estimated Chezy coefficient or Manning's n corresponding to the surface drag, and the geometric information of the tall vegetation and the associated

leaf canopies that may be present in the floodplain, the equivalent Chezy coefficient for over-bank flow can be estimated. Details of the derivation and the estimation of the Chezy coefficients are given in Appendix B.

3.3.2. Discharge calculation

Assuming both the main channel and floodplain to be hydraulically homogeneous, the common practice is to calculate the discharge in each section using a traditional open channel flow formula such as Chezy and Manning, and to arithmetically combine them to estimate total flow. However, in a study of interactions between the main channel and floodplain in a compound channel, Sellin (1964) showed that the presence of large velocity gradients between the main channel and floodplain can cause a shearing effect and consequent turbulent eddies. These can result in a momentum transfer from the faster moving fluid in the main channel to the slower moving fluid in the floodplain. Wormleaton and Merrett (1990) showed that ignoring the interactions at the main channel/floodplain interface can lead to large errors in the estimation of total discharges and the discharge components in the main channel and floodplain.

Radojkovic and Djordjevic (1985) introduced the so-called ϕ-index to quantify the effects of this momentum transfer between the main channel and floodplain, defined as the ratio of the boundary shear force to the gravitational force that drives the flow in each discharge component. This ratio is denoted by ϕ_m for the main channel and ϕ_f for the floodplain. Wormleaton and Merrett (1990) estimated the two ϕ-indices for their experimental set-up to be $\phi_m = 0.8$ and $\phi_f = 1.3$. Ervine and Baird (1982) proposed the following method to include the effects of this momentum transfer on the combined discharge (Q_t):

$$Q_t = Q_m \phi_m^{1/2} + Q_f \phi_f^{1/2} \quad (4)$$

where Q_m and Q_f are the isolated main channel and floodplain discharges given by any traditional friction formula, and ϕ_m and ϕ_f are the corresponding values of the ϕ-index.

4. Application of extreme flood model to the Collie River Basin

4.1. Study catchment

The Collie River Basin is located approximately 150 km south of Perth, in the south-west region of Western Australia (Fig. 3). The catchment area above the gauging station at Mungalup Tower is 2545 and 2845 km^2 just upstream of Wellington Dam. Because of previous application of the hillslope water balance model by Jothityangkoon et al. (2001), and the fact that no streamflow records are available for model validation at the Wellington Dam site following inundation by the dam, we implement the extreme flood model developed here only up to the Mungalup Tower site.

The landscape is characterised by gently undulating land with local relief varying from 50 to 150 m in the western part and less than 50 m in eastern part. The soils are predominantly gravelly and sandy laterites, 1–10 m thick, of high hydraulic conductivity, overlying deep kaolinitic sandy clay (about 30 m thick) of much lower hydraulic conductivity. The interpretation of the Landsat TM image (visible bands) of the catchment reveals that about 30% of the catchment area has been cleared for sheep grazing, cereal production and open cut mining. Over the uncleared areas, jarrah-marri forest is the dominant vegetation with some marri-wandoo and teatree woodlands in the valley floors. The region is subjected to Mediterranean climate with cool, wet winters (June–August) and warm to hot, dry summers (December–February). Annual average rainfall decreases from 1100 to 550 mm in the west to east direction, and annual average potential evaporation from the Class A pan also decreases from 1600 to 1400 mm in the same direction.

4.2. Parameter estimation for hillslope water balance model

As described in Jothityangkoon et al. (2001), the hillslope water balance model requires three sets of input variables and catchment parameters, relating to climate, soil and vegetation. Climatic inputs for the daily model are observed daily time series of rainfall and potential evaporation (e_p). Two types of soil

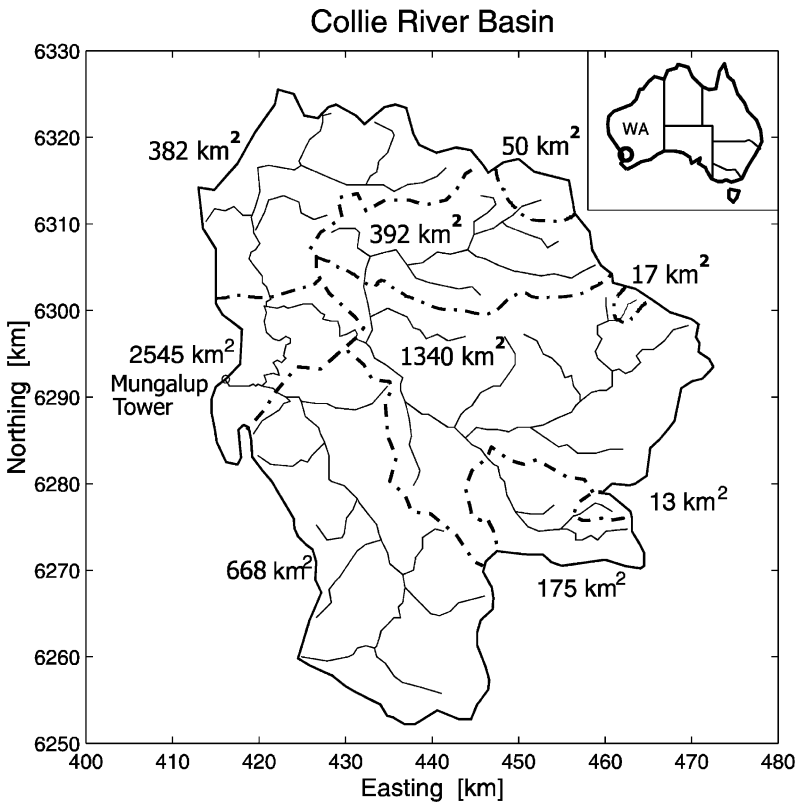

Fig. 3. Location map, stream network and boundaries of the Collie River Basin and a few study sub-catchments.

parameters are required, relating to the sizes of buckets (distribution of bucket capacities), and parameters related to the storage–discharge relationship for subsurface runoff. The bucket capacities are estimated from available maps of landforms, surveyed soil profile data corresponding to each of the landform types, and other soil hydraulic properties for soils in the south-west of Western Australia. The storage–discharge (recession curve) parameters relating to subsurface stormflow are determined from extensive analyses of observed recession curves. Using topography and the stream network, the study catchment is divided into 116 sub-catchments, and the above parameters have already been estimated a priori for each sub-catchment, as part of previous work.

When the model is applied in an hourly mode, measured hourly rainfall data is used as input. Because hourly e_p data is unavailable, daily e_p is divided by 24 to obtain the uniform hourly e_p values. We chose not to include more realistic diurnal variation of e_p as this level of complexity is not required for evaporation during flood events. The storage–discharge parameters relating to subsurface discharge flow are estimated again using recession analyses and the hourly runoff data, as a check on previous estimates. This led to fairly small changes to the previous parameter estimates. To determine the relationship between vertical hydraulic conductivity and water content for the estimation of the unsaturated zone delays, we use empirical equations presented by Clapp and Hornberger (1978), as outlined in Appendix A.

4.3. Parameter estimation for runoff routing model

Fig. 4(a) and (b) shows an illustration of the parameter estimation method based on surveyed channel cross-sections and the observed rating curve at station 612001 (1340 km^2) for sub-catchment No. 51. The first step is to estimate the effective

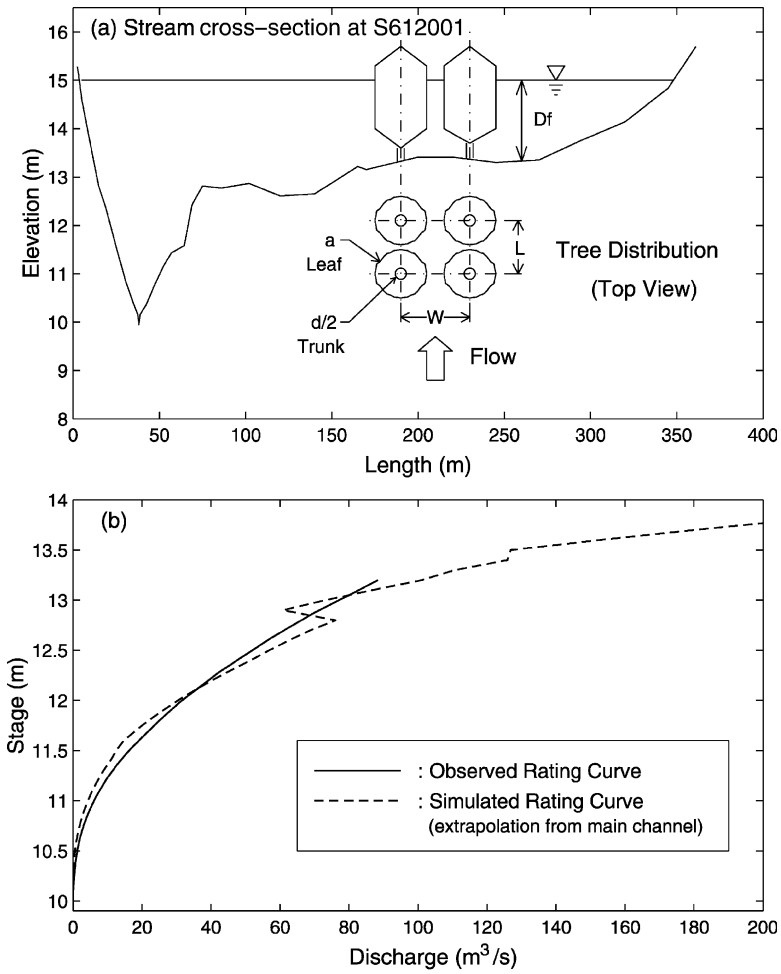

Fig. 4. An example of required hydraulic information at gauging station S612001 or sub-catchment No. 51: (a) parameters of tree distribution on floodplain and the surveyed channel cross-section, (b) comparison of the measured and simulated rating curves with extrapolation from main channel to include floodplain geometry but not vegetation ($S_f = 0.00011$, Manning's $n = 0.015$).

Chezy coefficient of the main channel, C_m. Given the channel cross-section in Fig. 4(a) and channel bed slope of 0.00011, a Manning coefficient ($n_m = 0.015$) is obtained first by fitting the simulated curve with the observed rating curve shown in Fig. 4(b), before converting to C_m.

As a first approximation, we assume that the Chezy coefficient relating to surface drag in the floodplain (due to bare soil, grasses and shrubs and bushes in the floodplain) is the same as that for the main channel, C_m. Later we will investigate the effect of using different Chezy coefficients for this surface drag on the estimated extreme discharges. In the second step, for each water level in a compound channel, the Chezy coefficient for the floodplain, C_f, the average velocity and the discharge are estimated from the previously known or assumed value of C_m. The distribution of trees in the floodplain was obtained from previous surveys conducted in the nearby Serpentine catchment by Deshon (1994), and representative values are presented in Table 1. The estimation procedure is described in detail in Section 3.2, summarised from Tamai (1992a,b).

For each water level, the discharges in both the main channel and floodplain sections are estimated separately: (i) Q_m, for the main channel—using

Table 1
Parameters for tree distribution on floodplain

Parameter	Value	Units
L	8.0	m
W	8.0	m
a	4.0	m
d	0.4	m
β	0.5	–

the empirical rating curve directly or indirectly using C_m, and (ii) Q_f, for the floodplain—using the estimated Chezy coefficient C_f. To account for the boundary shear between these two regions, these are combined together using Eq. (4). Results from hydraulic laboratory experiments carried out by Wormleaton and Merrett (1990) suggest that the ϕ-indices vary with water depth and the geometry of the compound channel. The magnitudes of ϕ_m become much less than unity with increase of floodplain width. However, there are no estimates of the ϕ-indices for the actual river reach used in this study catchment, or in any other actual river, which can be used as guidance. Therefore, as a first step, we decided to use the average ϕ-index values obtained from the laboratory experiments of Wormleaton and Merrett; $\phi_m = 0.8$ and $\phi_f = 1.3$, and assumed them to be constants for all depths. Clearly, much more work is required to arrive at appropriate values to be used under extreme flood conditions in actual river reaches.

Fig. 5(a) shows the estimated rating curves for four cases: (i) main channel only, i.e. existence of floodplain is ignored, (ii) compound channel (main channel and floodplain) but without explicit treatment of vegetation, i.e. extrapolation of rating curve of the main channel into the floodplain, assuming Manning's n remains constant regardless stage, (iii) compound channel, but with explicit treatment of vegetation, and identical Manning coefficients for the main channel and surface roughness of the floodplain ($n_f = n_m$), and (iv) compound channel with a higher surface roughness on the floodplain than on the main channel ($n_f = 2n_m$). These stage–discharge curves are converted to storage–discharge curves using average cross-sectional areas estimated from available topographic data, and the measured channel length for sub-catchment No. 51. The results are presented in Fig. 5(b). Two sets of the k and m parameters for in-bank (main channel) and over-bank flow (compound channel) are estimated by fitting power functions to the calculated storage–discharge curves, as shown in Fig. 5(b). We see that when vegetation effects on the floodplain are ignored with the assumption that $n_f = n_m$, the resulting exponent m is in the range 0.7–0.8, similar to the experimental results shown in Fig. 2(b) (geometry 1–4). On the other hand, with explicit treatment of vegetation on the floodplain, and the theory of compound channels, the exponent becomes closer to 1.0.

Table 2 presents the estimated k and m parameters of the routing model for 12 locations within the catchment—these correspond to existing streamflow gauging stations. It can be seen that in most cases, the storage–discharge curves of the compound channels are more linear ($m \approx 0.9$–1.0) than those of the main channel sections ($m \approx 0.7$–0.8). (This linearity is increased further when the roughness of the floodplain is increased further, such as when the Manning coefficient of the floodplain surface roughness is increased to twice that of the main channel (i.e. $n_f = 0.03$).) In three locations they remain non-linear and m remains roughly equal to that of the main channel; this is possibly due to the relatively small influence of floodplain inundation (sub-catchment nos. 63, 91 and 98). Apart from the sub-catchments in Table 2, observed rating curves and channel cross-sections are unavailable for the remaining 104 sub-catchments or river reaches. To estimate k and m parameters for each of these sub-catchments, a storage–discharge curve is constructed from available cross-sectional information, the rating curves available for neighbouring sub-catchments, localised channel lengths, and regionalised information on floodplain vegetation.

4.4. Application of rainfall–runoff model for PMF estimation

The hillslope water balance model representing runoff generation processes in sub-catchments is combined with the runoff routing model described previously (using the storage–discharge relationships estimated for compound channels), to

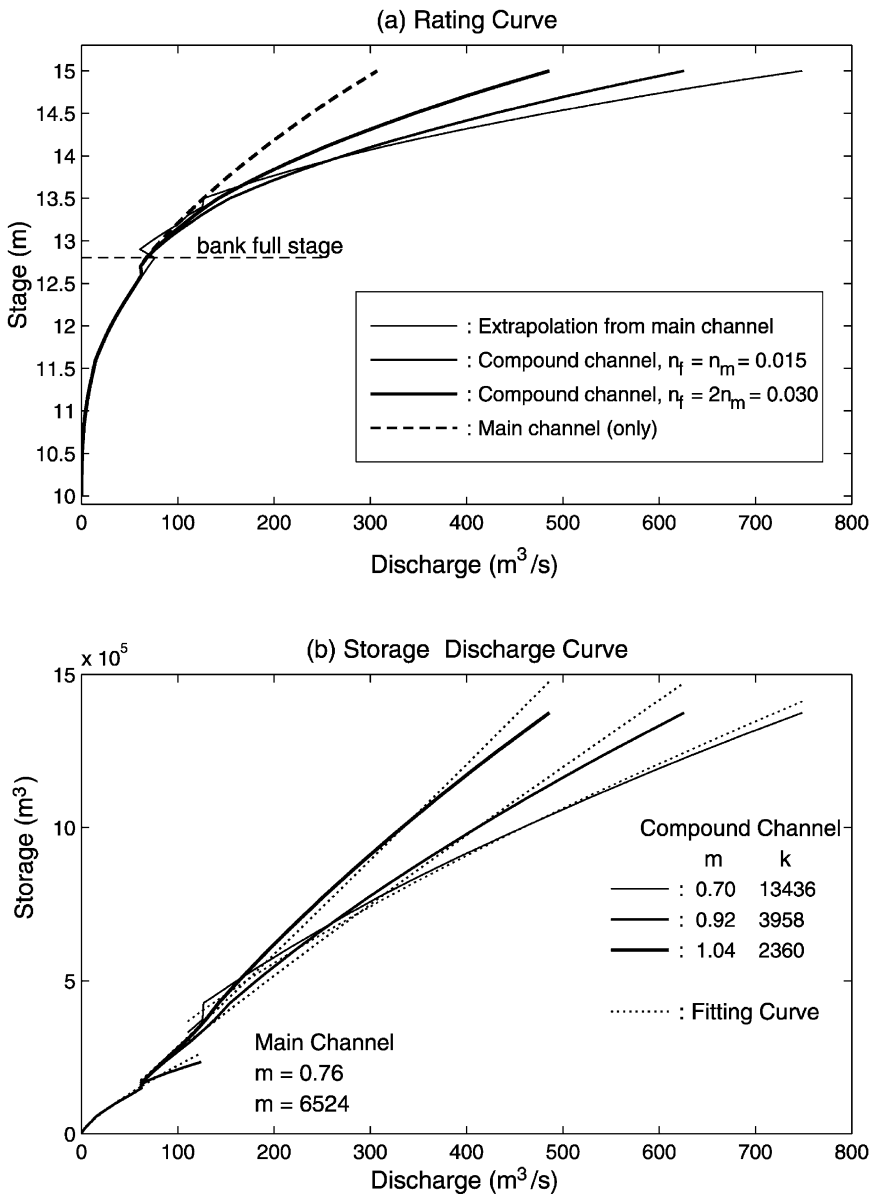

Fig. 5. An example of the estimated results for sub-catchment No. 51: (a) estimated rating curve for compound channel with $n_f = n_m = 0.015$, $n_f = 2n_m = 0.030$, and the extrapolation of main channel alone, (b) estimated storage–discharge curves and parameters k and m for in-bank and over-bank flows. NB: n_m and n_f denote the Manning coefficients for the main channel and floodplain, respectively.

simulate space-time fields of runoff in the river network. In this case the estimation is performed during extreme events (PMPs of specified duration and time of the year, e.g. winter or summer PMPs of duration, say, 24 h). The estimation process consists of three main steps:

(i) estimation of antecedent soil–water storage in the catchment prior to the storm event, by the application of the hillslope water balance model with a daily time step for a number of years up to the time of the particular event;

Table 2
Estimated parameters of the runoff routing model from calculated storage–discharge curves

Sub-catchment number	Site name	Site number	Catchment area (km^2)	Main channel		Compound channel ($n_f = n_m$)		Compound channel ($n_f = 2n_m$)	
				m	k	m	k	m	k
1	Mungalup Tower	S612002	2550.0	0.76	16,662	0.92	6189	0.99	3839
5	South Branch	S612034	668.0	0.76	4271	0.95	3138	1.10	2109
35	Tallanalla Road	S612017	382.0	0.76	1018	0.95	748	1.10	503
41	Scar Road	S612028	15.2	0.75	4003	0.88	3542	0.98	2834
51	Coolangatta Farm	S612001	1340.0	0.76	6524	0.92	3958	1.04	2360
63	Palmer	S612014	392.0	0.73	5499	0.68	9003	0.70	8878
77	Dons Catchment	S612007	3.5	0.76	2992	0.90	2810	1.01	2433
82	Stenwood	S612021	49.9	0.80	9047	0.93	6144	1.01	4585
91	James Well	S612025	175.1	0.70	4589	0.66	6183	0.68	5996
98	Maringee	S612026	12.8	0.78	6665	0.69	15,936	0.72	14,946
105	James Crossing	S612230	169.0	0.76	7414	1.06	2921	1.20	1846
110	Maxon Farm	S612016	16.6	0.74	15,219	0.90	17,100	1.07	13,198

(ii) transformation of rainfall hyetograph to a rainfall excess hyetograph (rate of runoff generation), corresponding to the chosen PMP, in each sub-catchment using the hillslope water balance model, but using an hourly time step;
(iii) estimation of the PMF at the catchment outlet using the runoff routing model, with the rainfall excess hyetographs estimated earlier being the sub-catchment inputs to the stream channel network.

4.5. Model validation

It is important to note that the PMF is a very rare extreme event, which is beyond what is available in the historical record. Therefore, estimates of the PMF can never be validated fully. All we can hope to do is to validate components of the rainfall–runoff model on different datasets, and the combined model on some less-than-extreme flood events, but the key at all times is that estimation of parameters should not be based on calibration on less-than-extreme flood events. The limited model validation exercises should be combined with sensitivity analyses with respect to model parameters to determine the mechanisms that may contribute to extreme floods and estimate the uncertainty in the model predictions.

As mentioned before, the hillslope water balance model was developed previously with minimal calibration on this same catchment, and has been shown to produce a good match to the observed runoff record. This has been presented in detail in Jothityangkoon et al. (2001), and will not be presented here. The combined water balance and routing model has been used to predict the short-term (hourly) response to a large event in July 1990, as a way of validating the combined model during individual events. Fig. 6 shows a comparison between observed and simulated discharges for two sub-catchments of the Collie catchment. As suggested earlier, the antecedent soil moisture was prescribed using a previous application of the daily model up to July 1990. There has been minimal calibration involved in the estimation of the model parameters, except for the use of recession analysis for the estimation of two parameters, and for the above specification of antecedent conditions. It is clear that the predicted hydrograph represents a good match to the observed one, in terms of both the general shape and the magnitude and timing of the flood peaks. Considering that both the runoff generation component and the routing component have explicitly allowed for a possible extrapolation to extreme flood events, the model can therefore be used with some confidence to estimate the PMF. Any errors in the model predictions

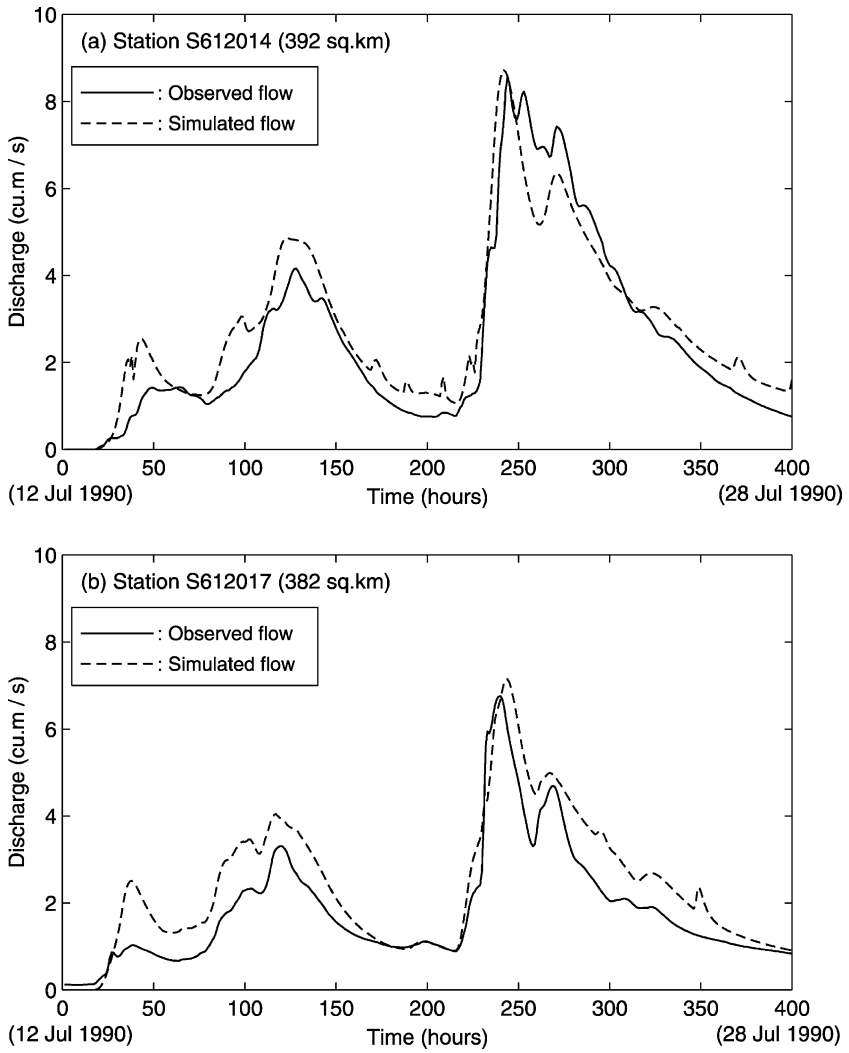

Fig. 6. Comparison of observed and simulated discharges for a storm in July 1990: (a) at gauging station S612014 (392 km^2), (b) at gauging station S612017 (382 km^2).

of the PMF relate to the physical bases of the extrapolations, and the estimation of parameters involved.

4.6. PMP for the Collie River Basin

The estimates of the PMP used in this study were derived from the Generalised Tropical Storm Method (GTSM) by the Australian Bureau of Meteorology's Hydrometeorological Advisory Service (Bureau of Meteorology, 1996). The estimated PMP values of durations ranging from 6 to 72 h for the Collie River Basin are listed in Table 3. The time series of PMP intensities (i.e. hyetographs) for each duration and each sub-catchment are generated as an input to the distributed rainfall–runoff

Table 3
PMP estimates for Wellington Dam Catchment by Generalised Tropical Storm Method (after Pearce (1996))

Duration (h)	12	18	24	36	48	72
PMP (mm)	390	500	570	630	670	740

model, using the temporal patterns and spatial distributions of PMPs which are recommended by Bureau of Meteorology (1996).

5. Results and discussion

5.1. Estimated PMFs under different conditions

The results of the transformation of PMPs to PMFs using the rainfall–runoff model for the Collie catchment up to Mungalup Tower (2545 km^2) are shown in Table 4. The estimated PMFs are used towards the following investigations:

(i) use of different routing parameters for the compound channel (using two sets of m and k values for in-bank and over-bank flows, respectively), and for the extrapolation of the main channel (the same set of m and k values for both flows);
(ii) effects of different durations;
(iii) the effects of antecedent catchment wetness, i.e. the effects of winter and summer conditions;
(iv) sensitivity study on the effects of higher surface roughness on the floodplain and a shallower soil depth distribution;
(v) estimates of the PMF for different locations and for different catchment sizes.

The results of these investigations are presented below.

The use of routing parameters estimated from compound channels always give a lower PMF estimate, except for some small sub-catchments in which the dominant runoff process did not change from in-bank flow to over-bank flow. This shows that the effect of floodplain resistance during over-bank flow tends to reduce the magnitude of the PMF. Testing with five different durations of the PMPs suggested that the maximum PMF is obtained for 24 h duration storms at all locations. By using the same temporal and spatial patterns and the same total depth of PMP, PMF estimates in winter are always higher than in summer due to higher antecedent wetness of the catchments in winter. The increase of surface roughness in the floodplain, i.e. $n_f = 2n_m$ retards the flow in the compound channel and causes a ~20% reduction in the PMF. The reduction of mean soil depth by 25% tends to increase the PMF by ~40%.

5.2. PMF and expansion of saturated area

Fig. 7 presents the distributions of bucket capacity and soil moisture storage for two sub-catchments in central and eastern Collie, generated by the distributed rainfall–runoff model. Firstly, a comparison of the storage capacities between the two sub-catchments (solid line) shows that the soils in central Collie are deeper than in eastern Collie. As a consequence of receiving the PMP, water storages in both sub-catchments have increased, and this increase is larger than the maximum range of water storage values (maximum–minimum) obtained by the application of the continuous water balance over many years. This increase of soil water storage is seen to cause the expansion of the saturated area fraction in central Collie from about 5% (under normal floods) to about 20% (under extreme rainfall), as shown in Fig. 7(a). The eastern Collie also shows a similar increase of saturated area fraction (Fig. 7(b)). A consequence of the increased saturation area is a corresponding increase of saturation excess overland flow during extreme flood events.

Note that the small saturation areas obtained are a result of the deep soils in this region, with average depth assumed to be in the range of 2.5–3.0 m. Smaller soil depths will certainly result in larger saturation area fractions and higher flood peaks, as demonstrated in Table 4(d). Clearly, the model is highly sensitive to soil depths, and the simulations highlight the need to estimate these more carefully.

5.3. PMF and floodplain inundation

The estimated PMFs for sub-catchment No. 51 (1340 km^2) in Table 4(a) shows that the PMF in winter condition is always larger than 2000 m^3/s for all durations. This PMF can be converted to a flow stage (water level height) in the channel using the estimated rating curve shown in Fig. 5(a). It can be seen that the estimated PMF is very large indeed, extending far beyond the limit of even the estimated rating curve (i.e. 700 m^3/s), let alone the observed one. Indeed, the water level in the stream channel

Table 4
Estimated PMFs for winter and summer conditions at 5 locations in the Collie River Basin from PMPs with different durations: (a) using parameters which include the effects of floodplains and $n_f = n_m$, (b) using parameters extrapolated from the main channel, (c) using parameters which include the effects of floodplains and $n_f = 2n_m$, and (d) using parameters which include the effects of floodplains, $n_f = n_m$, and the decrease of mean soil depth by 25%

Sub-catchment number		PMF (m^3/s) from different durations of PMP				
		12 h	24 h	36 h	48 h	72 h
(a)						
1	Winter	2454.7	4285.0	4263.0	3886.3	3600.9
(2550 km^2)	Summer	1166.1	1713.0	1858.5	1741.8	1591.9
51	Winter	2158.3	2901.1	2791.7	2489.7	2279.1
(1340 km^2)	Summer	952.9	1283.0	1332.6	1208.7	1097.2
63	Winter	344.3	406.5	351.3	283.9	270.7
(392 km^2)	Summer	184.2	207.2	142.1	116.8	112.0
82	Winter	18.4	17.6	13.2	11.7	11.3
(50 km^2)	Summer	4.7	7.1	5.3	4.4	4.1
110	Winter	28.8	29.2	25.4	20.9	20.0
(17 km^2)	Summer	8.8	11.4	10.2	9.1	8.2
(b)						
1	Winter	4092.5	6024.2	5609.9	4773.7	4388.3
(2550 km^2)	Summer	1752.8	2397.1	2381.4	2130.8	1855.3
51	Winter	3204.8	3801.8	3488.8	2822.6	2640.8
(1340 km^2)	Summer	1419.3	1713.2	1644.0	1368.7	1194.7
63	Winter	442.6	483.0	362.8	298.8	277.8
(392 km^2)	Summer	236.1	254.0	154.4	130.9	125.0
82	Winter	18.4	17.6	13.2	11.7	11.3
(50 km^2)	Summer	4.7	7.1	5.3	4.4	4.1
110	Winter	37.1	32.8	26.4	22.7	21.8
(17 km^2)	Summer	8.8	15.3	12.3	9.1	8.2
(c)						
1	Winter	2029.3	3491.4	3648.1	3453.1	3217.6
(2550 km^2)	Summer	922.0	1415.9	1607.4	1572.6	1453.7
51	Winter	1761.1	2521.3	2451.4	2235.9	2073.0
(1340 km^2)	Summer	787.4	1140.6	1204.2	1121.3	1025.1
63	Winter	328.1	377.2	340.1	280.9	263.2
(392 km^2)	Summer	157.5	185.8	139.7	113.6	106.9
82	Winter	18.4	17.6	13.2	11.7	11.3
(50 km^2)	Summer	4.7	7.1	5.3	4.4	4.1
110	Winter	25.1	27.0	24.2	20.2	19.0
(17 km^2)	Summer	8.7	10.6	9.8	9.1	8.2
(d)						
1	Winter	3735.5	5986.3	5811.0	5338.6	4949.6
(2550 km^2)	Summer	1467.4	2424.1	2628.7	2474.5	2245.1
51	Winter	3316.0	4016.9	3697.3	3267.3	3049.0
(1340 km^2)	Summer	1230.6	1947.0	1915.1	1723.9	1555.4
63	Winter	606.7	557.7	488.1	405.8	384.5
(392 km^2)	Summer	246.2	246.2	227.4	177.0	156.5
82	Winter	28.6	18.6	14.9	12.9	12.7
(50 km^2)	Summer	8.0	8.6	6.6	5.8	5.5
110	Winter	38.6	40.9	35.5	29.0	27.4
(17 km^2)	Summer	13.1	16.6	15.0	12.6	11.1

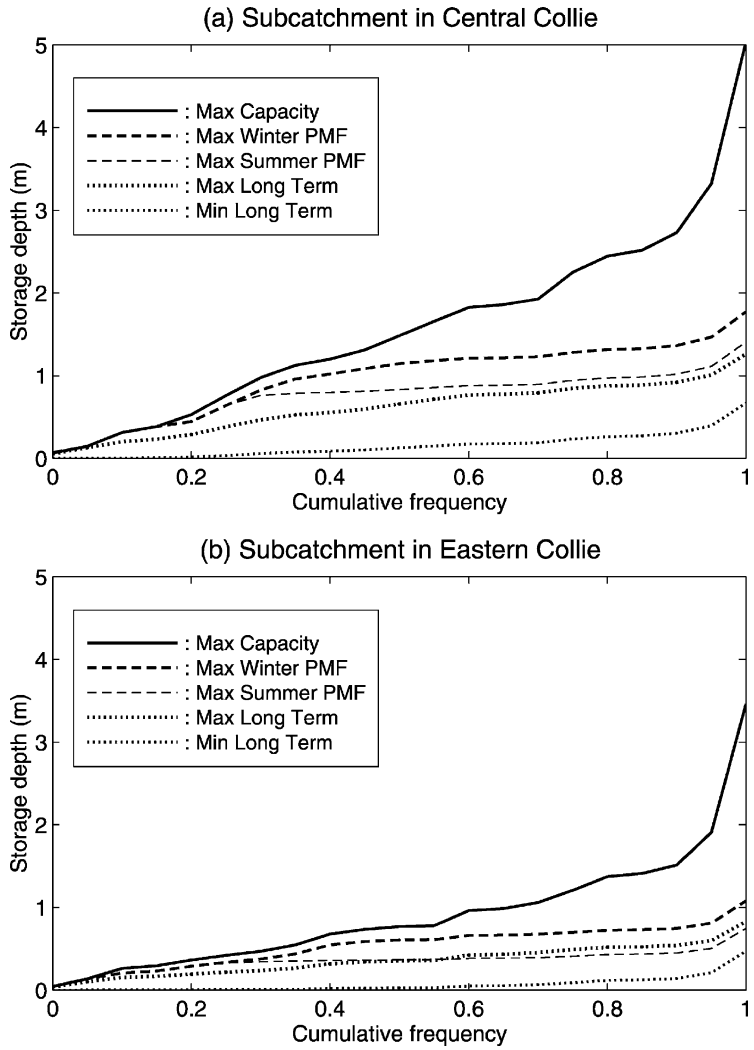

Fig. 7. Change in soil moisture storage in a sub-catchment relative to storage capacity: maximum and minimum long-term storage distribution obtained from the daily water balance model, and the maximum storage in winter and summer conditions as the result of the application of the PMP: (a) sub-catchment in central Collie, (b) sub-catchment in eastern Collie.

resulting from the application of the PMP extends even beyond the surveyed channel cross-section.

If the side slope of the channel is extrapolated to accommodate 2000 m^3/s, the increase of water level could be as much as 3.5 m above the current highest stage (15 m) in the surveyed channel cross-section. In comparison, in-bank flow remains the dominant runoff process only if discharge stays below the very small amount of 90 m^3/s, as shown in Fig. 5(a). Even while not doubting that over-bank flow will be the dominant runoff process under extreme flood conditions, it is clear that the extrapolation we have used is still very tentative. There is a clear need for a detailed survey of cross-sectional geometry and floodplain vegetation up to about 4 m above the maximum stage used here.

5.4. Comparison to PMF estimates from the RORB model

The PMF estimates for the Collie River Basin at Wellington Dam have been previously reviewed by

Table 5
Comparison of PMF estimates by the Water and Rivers Commission (using RORB model) and estimates from this study (main channel extrapolation, compound channel with $n_f = n_m$ and observed soil depth distribution, compound channel with $n_f = 2n_m$ and observed soil depth distribution, compound channel with $n_f = n_m$ and the decrease of mean soil depth by 25%)

	Probable maximum flood (m^3/s)			
Duration of PMP (h)	12	24	48	72
Water and Rivers Commission[a]	2420	5585	6190	5760
This study[b] (a) main channel extrapolation	4092	6024	5610	4388
(b) including floodplain inundation, $n_f = n_m$	2455	4285	3886	3600
(c) including floodplain inundation, $n_f = 2n_m$	2029	3491	3453	3218
(d) including floodplain inundation, $n_f = n_m$ and shallower soil depths	3736	5986	5339	4950

[a] At Wellington Dam inflow (2845 km^2).
[b] At Mungalup Tower (2550 km^2).

the Western Australian Water and Rivers Commission (WRC) (Pearce, 1996). This study used the RORB model (Laurenson and Mein, 1988), which is the current standard approach used for extreme flood estimation. However, unlike standard practice, this study utilised the SWMOD model (Stokes, 1989) for estimating the rainfall excess.

Table 5 presents a comparison between the PMFs estimated by the WRC and those estimated during this study. The critical duration for the PMF determined by WRC was 48 h, which is higher than the 24 h estimated in our study. Interestingly, however, when the runoff routing parameters are extrapolated based on the main channel only, the highest magnitude of PMF from the WRC study is only slightly higher than that estimated in this study.

Exact comparison between the two estimates is precluded because the present study is based on application of a rainfall–runoff model calibrated with streamflow data observed at Mungalup Tower, rather than at Wellington Dam site. Some of the differences can therefore be explained by the increase in catchment area used (Mungalup Tower, 2545 km^2 versus Wellington Dam, 2845 km^2). Nevertheless, useful inferences can indeed be made about the methods since the differences in catchment areas is less than 12%.

The good agreement between the two estimates in this case is reassuring in that the runoff generation components in both models were derived from the same soil depth distributions, and both models used aspects of the main channel hydraulics but incorporated them differently. In the WRC study, the inclusion of channel hydraulics was indirectly based on calibration with actual flood events, whereas in our study they were derived directly from empirical rating curves, and verified on actual flood events.

When our runoff routing model included the effects of floodplain inundation and the effects of floodplain vegetation, the maximum PMF estimates decreased from 6024 to 4285 m^3/s, or 30% less than the estimates obtained by the WRC study and by our model with extrapolation of the main channel alone. Sensitivity analyses with respect the surface roughness in the floodplain showed that a doubling of the surface roughness, i.e. $n_f = 2n_m$, reduced the PMF by a further ~20%. These results clearly show that if the effects of floodplain geometry and vegetation are included, they lead to a major reduction in the estimated PMFs. A similar sensitivity study with respect to soil depth distribution showed that a 25% reduction of the mean soil depth caused a 40% increase in the PMF, from 4285 to 5986 m^3/s. These results could have major ramifications for future estimation of extreme floods in the region, and for the safety of existing dams and other structures, which have been designed on the basis of previous standard estimates.

6. Conclusions

By using a distributed water balance model, this paper has demonstrated the potential for a major change of dominant runoff processes and to the streamflow rating curve when moving from normal floods to extreme floods. Firstly, there is a substantial increase in saturation excess overland flow, through

the expansion of saturated area fractions due to the saturation of soil profiles in shallower soils. Secondly, there is enormous potential for over-bank flow to take over from in-bank or main channel flow during extreme flood events. Over-bank flow is controlled by geometry of the compound channels, the vegetation cover and other roughness elements on the floodplains, and interactions between main channel flows and floodplain flows.

The distributed water balance model developed in this study consists of a hillslope water balance model, which simulates the runoff generation processes on hillslopes, and a distributed runoff routing model representing flow process in a composite channel, which is described in terms of a non-linear storage–discharge relationship. The model contains a number of physical parameters, which are all estimated a priori with little or no calibration. This model is used to transform estimates of PMP to estimates of PMF in the Collie catchment, and has been shown to provide reasonable results in comparison with magnitudes of PMF estimated by the Water and Rivers Commission in a standard manner using the RORB model. The simulation results show that estimated PMF values will be smaller if the effects of floodplain inundation and vegetation cover on floodplains are included, and suggest that the current estimates of PMF by the WRC may need careful re-evaluation.

A major advantage of the model presented in this paper is that it has the capability to evaluate the effects of physical changes in a catchment on the PMF, such as the change of channel cross-section geometry, vegetation cover on floodplains and the effects of deforestation within sub-catchments. However, the model has not considered runoff generation by infiltration excess overland flow, which may arise if large parts of the catchment lose their current vegetation cover leading to compaction of the soils—this may enhance the generation of infiltration excess runoff.

As mentioned, estimated water levels during extreme flood events will exceed the spatial extent of the surveyed cross-sections, which were used in the study. Clearly, surveying of the cross-sections should be carried further up the hillslopes at a number of locations so as to give a very good regional coverage of floodplain characteristics. This should be combined with a quantitative survey of vegetation cover on the hillslopes and near the channel. These are needed to construct revised rating curves across this catchment, and in other catchments in the region, for extreme flood estimation purposes. Finally, more work should be carried out to obtain reliable estimates of soil depths, especially near the stream zone, so as to obtain more accurate estimates of saturation excess overland flow.

In conclusion, the work presented has left the authors in awe of the tremendous extrapolations required, both in terms of our understanding of likely processes, and the appropriateness of the parameter values used, in the estimation of extreme floods. While the models used and the specific processes described in this paper are specific to Western Australia and cannot be extrapolated to other regions, the methods we adopted to deal with change of processes can benefit other hydrologists elsewhere. Extreme floods are phenomena that lie clearly beyond the level of normal human comprehension, and their estimation must always be treated with caution. At a philosophical level, it would seem wise to use simple, intuitive models, rather than complex models that are too closely tied to human experiences gained at small spatial scales and low return periods.

Acknowledgements

The authors are grateful to John Ruprecht and Bradley Fuller (Water and Rivers Commission) for their assistance in providing field data and previous flood study reports for the Collie River Basin. We wish to acknowledge the Royal Thai Government for financial support in the form of a PhD Scholarship to the first author. The second author thanks the Water and Rivers Commission, and the former Water Authority of Western Australia, for their financial and technical support towards this project in previous years.

Appendix A. Hillslope water balance model with unsaturated zone delay

The original daily water balance equation for a single bucket is given by (Jothityangkoon et al., 2001):

$$\frac{\mathrm{d}s(t)}{\mathrm{d}t} = i(t) - e_{\mathrm{b}}(t) - e_v(t) - q_{\mathrm{ss}}(t) - q_{\mathrm{se}}(t) \qquad \text{(A1)}$$

where $s(t)$ is the volume of lumped soil water storage, $i(t)$ is precipitation intensity, $e_b(t)$ is bare soil evaporation, e_v is transpiration, q_{se} is saturation excess runoff rate, and q_{ss} is subsurface runoff. To incorporate delay in the unsaturated zone, s is separated into saturated storage, s_s, and unsaturated storage, s_u. The water balance equations for s_u and s_s are given by:

$$\frac{ds_u(t)}{dt} = i(t) - e_b(t) - e_{v1}(t) - q_i(t) - q_{se}(t) \quad \text{(A2)}$$

$$\frac{ds_s(t)}{dt} = q_i(t) - e_{v2}(t) - q_{ss}(t) \quad \text{(A3)}$$

where $q_i(t)$ is outflow rate from s_u to s_s. In this case, because the model is only operated during or immediately after storm events, e_{v1} and e_{v2} are formulated such that $e_{v1} + e_{v2}$ is equal to potential transpiration rate $k_v Me_p$ (see Jothityangkoon et al. (2001)). When the unsaturated zone cannot deliver the potential transpiration rate, water is extracted from the saturated store. The capacity of the unsaturated storage, s_{ub}, is a part of total storage capacity, S_b, and can be described by

$$s_{ub} = S_b - s_s \quad \text{(A4)}$$

Internal flow rate q_i can be expressed as a function of hydraulic conductivity, K_h, and the hydraulic gradient, and K_h can be approximated as a function of saturated hydraulic conductivity, K_{hsat} and the degree of saturation, S, $S = s_u/s_{ub}$:

$$q_i = K_h\left(1 + \frac{i\Delta t}{s_{ub}}\right) \quad \text{(A5)}$$

$$K_h = K_{hsat}S^c \quad \text{(A6)}$$

$$c = 2b + 3 \quad \text{(A7)}$$

where Δt is the time step = 0.5 h. Note that in the spirit of the Green–Ampt equation, the first term on the RHS of Eq. (A5) refers to a gravitational component and the second terms refers to a capillary component. Typical soil texture in Collie is sandy loam, so we use $b = 4.9$ (Clapp and Hornberger, 1978), and $K_{hsat} = 3.47 \times 10^{-3}$ cm/s or 125 mm/h.

Appendix B. Flow resistance for one-dimensional over-bank flow

B.1. Theoretical derivation of form drag

To estimate the Chezy coefficient and the average velocity of over-bank flow in the floodplain, the whole floodplain area is divided into two sections: treed and non-treed. The sectional average velocities in the treed area (U_{fot}) and in the non-treed area (U_{fof}) are estimated separately and combined to estimate the average velocity for the whole floodplain (U_{fo}), using the fraction of treed area in the floodplain (β_S) as a weighting parameter. The surface resistance coefficient needed for the estimation of U_{fof} is initially assumed to be the same as that of the main channel.

For estimation of U_{fot}, Tamai (1992a,b) assumed that the actual distribution of trees in the floodplain can be simulated by groups of vertical circular columns with diameter d. The form drag of a single column (F_{D1}) is given by

$$F_{D1} = C_D D_f d \frac{\rho}{2} U_{fot}^2 \quad \text{(B1)}$$

where C_D is drag coefficient, D_f is water depth on the floodplain, ρ is density of water, and U_{fot} is sectional average velocity in treed area of floodplain flow. For the formulation of form drag caused by coherent eddy patches, the longitudinal velocity in the patches that are formed around the trees is assumed to be zero. Assuming steady state, the average number of coherent eddy patches remains unchanged and the rate of generation and dissipation of the patches is roughly equal. The form drag caused by such macro-scale turbulence (F_{D2}) is described by

$$F_{D2} = \rho\pi a^2 D_f \frac{U_{fot}}{T} \quad \text{(B2)}$$

where a is representative radius of a coherent eddy patch assumed to be equal to the radius of leaf–branch complex, and T is representative period of generation of the coherent eddy patches. These are also called macro-scale bursts, and are boils formed in the wake of branch–leaf complexes of trees.

Using a relationship between bed shear stress and the Chezy formula, the surface drag caused by surface roughness can be derived from the longitudinal

component of the bed shear stress (τ_{bx}) and the effective flow area,

$$F_{SD} = \tau_{bx} A' LW \tag{B3}$$

$$F_{SD} = A' LW \rho g U_{fot}^2 / C_m^2 \tag{B4}$$

where A' is effective flow area, L is longitudinal interval of trees, W is transverse interval of trees, g is acceleration of gravity, and C_m is the common Chezy coefficient assumed for both the main channel and the floodplain, and linked to a Manning's coefficient n_m (in this case, we will also investigate the effects of any relaxation of this assumption).

The driving force from gravity due to the effective water mass (F_G) is given by

$$F_G = (\rho A' LW D_f) g S_0 \tag{B5}$$

$$A' = 1 - 2al_b/W \tag{B6}$$

where S_0 is longitudinal hydraulic gradient of floodplain, and l_b is leaf block or partial block ratio.

Applying the linear momentum equation in the flow direction, the gravity force due to the water mass (F_G) is balanced by a combination of resistance forces from the actual form drag caused by tree trunks (F_{D1}), the form drag due to macro-scale turbulence (F_{D2}), and that due to surface roughness (F_{SD}),

$$F_G - (F_{D1} + F_{D2} + F_{SD}) = 0 \tag{B7}$$

Substituting Eqs. (B1), (B2), (B4), (B5) into Eq. (B7) and dividing by $\rho g A' LW$ yields

$$D_f S_0 - \frac{C_D}{2g} \frac{D_f d}{A' LW} U_{fot}^2 - \frac{\pi a^2}{A' LW} \frac{D_f U_{fot}}{gT} - \frac{U_{fot}^2}{C_m^2} = 0 \tag{B8}$$

Not much is known about the properties of macro-scale bursts in the wake of trees, and Tamai's work brings together existing knowledge on micro-scale and (intermediate) meso-scale bursts to offer an approximate estimate of T. Let us denote by T_B the representative period of generation micro-scale bursts. It was found for open channel flow experiments that the ratio of $T_B U_{max}/D_f$ or α_P is about 1.5–3 where U_{max} is the maximum velocity at the water surface.

Even though not much is known about the relationship between T and T_B, Tamai assumed a linear relationship $T = \alpha_B T_B$. This gives rise to:

$$T = \frac{\alpha_B \alpha_P}{\alpha_S} \frac{D_f}{U_{fot}} \tag{B9}$$

where

$$\alpha_S = U_{max}/U_{fot} \tag{B10}$$

and

$$\alpha_B = T/T_B \tag{B11}$$

Substituting Eq. (B9) into Eq. (B8) yields

$$D_f S_0 - \frac{U_{fot}^2}{C_m^2} \left[C_D \beta_t \frac{C_m^2}{2g} + \beta_b \frac{\alpha_S}{\alpha_B \alpha_P} \frac{C_m^2}{g} + 1 \right] = 0 \tag{B12}$$

where

$$\beta_t = \frac{D_f d}{A' LW} \tag{B13}$$

$$\beta_b = \frac{\pi a^2}{A' LW} \tag{B14}$$

Rearranging Eq. (B12) to obtain the average velocity of uniform flow in the treed area of the floodplain, we obtain:

$$U_{fot} = \frac{C_m \sqrt{D_f S_0}}{\sqrt{1 + K_1 + K_2}} = C_{ft} \sqrt{D_f S_0} \tag{B15}$$

where

$$K_1 = (C_m^2/2g) C_D \beta_t \tag{B16}$$

$$K_2 = (C_m^2/g)(\beta_b \alpha_S / \alpha_P \alpha_B) \tag{B17}$$

Here, C_{ft} is the equivalent Chezy coefficient for over-bank flow in the treed region, K_1 is the ratio of form drag caused by tree trunks to the surface drag, and K_2 is the ratio of form drag caused by coherent eddy patches to the surface drag.

The average velocity for the whole over-bank flow (U_{fo}) is a combination of average velocity in the non-treed area (U_{fof}) and the average velocity in the treed area (U_{fot}), with respect to the ratio of the treed area and total area normal to over-bank flow in floodplain (β_S),

$$U_{fo} = (1 - \beta_S) U_{fof} + \beta_S U_{fot} \tag{B18}$$

Substituting the velocities using the original Chezy formula, namely $U_{fo} = C_f \sqrt{D_f S_0}$, $U_{fof} = C_m \sqrt{D_f S_0}$, and U_{fot} in Eq. (B15) into Eq. (B18) (and assuming

that the resistance coefficient on the floodplain is the same as in the main channel), yields the Chezy coefficient for the whole over-bank flow,

$$C_f = C_m\left[(1-\beta_S) + \frac{\beta_S}{\sqrt{1+K_1+K_2}}\right] \tag{B19}$$

B.2. Coefficient estimation for over-bank flow

To estimate the dynamic coefficients in Eqs. (B16) and (B17) for use in Eq. (B19), the relationship between the period of burst generation of a macro-scale boil described in Section B.1 (T) and that of a meso-scale bursts (T_M), in the lee of ripples behind sand dunes, etc. and obtained from laboratory experiments, is essential. Existing knowledge of meso-scale bursts suggests that the average observed period of the generation of burst (vortex) behind the ripples (T_M) can be formulated as,

$$T_M = 7.5\frac{D_f}{U_{fot}} \tag{B20}$$

The ratio of average period of generation between meso-scale and macro-scale bursts is then given by,

$$\frac{T_M}{T_B} = \frac{7.5D_f/U_{fot}}{\alpha_P D_f/U_{max}} = \frac{7.5\alpha_S}{\alpha_P} \tag{B21}$$

Using a logarithmic velocity profile for open channel flow velocity in Eq. (B10), α_S can be approximately estimated to be 1.2. Typical value of α_P is 2 (Nakagawa and Nezu, 1981). Assuming that the ratio between the periods of macro-scale bursts (T) and meso-scale bursts (T_M), remains the same as that given by Eq. (B21), we have $\alpha_B = (7.5\alpha_S/\alpha_P)^2$, This then gives:

$$\frac{\alpha_S}{\alpha_B\alpha_P} = \frac{\alpha_S}{(7.5\alpha_S/\alpha_P)^2\alpha_P} = 3.0\times10^{-2} \tag{B22}$$

The typical drag coefficient (C_D) for the treed region is set to be 1.5, measured values of C_D in a half width of channel covered by a staggered array of piles is in the range of 1–2. Substituting the values of C_D and Eq. (B22) in Eqs. (B16) and (B17) gives,

$$K_1 = 0.75\beta_t\left(\frac{C_m^2}{g}\right) \tag{B23}$$

$$K_2 = 3.0\times10^{-2}\beta_b\left(\frac{C_m^2}{g}\right) \tag{B24}$$

These are substituted back in Eq. (B19) for the estimation of the effective Chezy coefficient for floodplain flows. More details of the estimation for over-bank flow can be found in Tamai (1992a,b), and its application to the nearby Serpentine catchment is presented in Deshon (1994).

References

Bates, B.C., Pilgrim, D.H., 1983. Investigation of storage–discharge relations for river reaches and runoff routing models. Civ. Engng Trans., Inst. Engrs Aust. CE25 (3), 153–161.

Bates, B.C., Pilgrim, D.H., 1986. Simple models for nonlinear runoff routing. Civ. Engng Trans., Inst. Engrs Aust. CE28 (4), 284–291.

Boyd, M.J., Pilgrim, D.H., Cordery, I., 1979. A storage routing model based on catchment geomorphology. J. Hydrol. 42, 209–230.

Bureau of Meteorology, 1996. Generalised probable maximum precipitation estimates for the Wellington Dam catchment. Report No. GPMP/11, Hydrometeorological Advisory Service, Bureau of Meteorology, Melbourne.

Clapp, R.B., Hornberger, G.M., 1978. Empirical equations for some soil hydraulic properties. Water Resour. Res. 14, 601–604.

Deshon, C.J., 1994. Improved Characterisation of River Channel Hydraulics for Flood Estimation. BE Honours Thesis, Department of Civil Engineering, University of Western Australia, Crawley.

Ervine, D.A., Baird, J.I., 1982. Rating curves for rivers with overbank flow. Proc. Inst. Civ. Engrs London 73 (2), 465–472.

Foufoula-Georgiou, E., 1989. A probabilistic storm transposition approach for estimating exceedance probabilities of extreme precipitation depths. Water Resour. Res. 25 (5), 799–815.

Jothityangkoon, C., Sivapalan, M., 2001. Temporal scales of rainfall–runoff processes and spatial scaling of flood peaks: space-time connection through catchment water balance. Adv. Water Resour. 24, 1015–1036.

Jothityangkoon, C., Sivapalan, M., Farmer, D.L., 2001. Process controls of water balance variability in a large semi-arid catchment: downward approach to hydrological model development. J. Hydrol. 254, 174–198.

Klemes, V., 1993. Probability of extreme hydrometeorological events—a different approach. In: Kundzewicz, Z.W., Rosbjerg, D., Simonovic, S.P., Takeuchi, K. (Eds.), Extreme Hydrological Events: Precipitation, Floods, Droughts, IAHS Publ. No. 213, pp. 167–176.

Kölla, E., 1987. Estimating flood peaks from small rural catchment in Switzerland. J. Hydrol. 95, 203–225.

Laurenson, E.M., Mein R.G., 1988. RORB—Version 4 Runoff Routing Program User Manual, Department of Civil Engineering, Monash University, p. 186.

Menabde, M., Sivapalan, M., 2001. Linking space-time variability of river runoff and rainfall fields: a dynamical approach. Adv. Water Resour. 24, 1001–1014.

Nakagawa, H., Nezu, I., 1981. Structure of space-time correlation of bursting phenomena in an open-channel flow. J. Fluid Mech. 104, 1–43.

Pearce, L.J., 1996. Collie river flood study. Report No. SWH8 1997, Surface Water Hydrology Series, Water and Rivers Commission.

Pilgrim, D.H., Rowbottom, I.A., 1987. Estimation of large and extreme floods. In: Pilgrim, D.H. (Ed.), Third ed, Australian Rainfall and Runoff: A Guide to Flood Estimation, vol. 1. Institute of Engineers Aust., Canberra, Chapter 13.

Radojkovic, M., Djordjevic, S., 1985. Computation of discharge distribution in compound channels, In: Proceedings of 21st Congress, International Association for Hydraulic Research, Melbourne, Australia, vol. 3., pp. 367–371.

Sellin, R.J.H., 1964. A laboratory investigation into the interaction between flow in the channel of a river and that of its floodplain. La Houille Blanche 7, 793–801.

Sivapalan, M., Wood, E.F., Beven, K.J., 1990. On hydrologic similarity. 3. A dimensionless flood frequency model using a generalised geomorphic unit hydrograph and partial area runoff generation. Water Resour. Res. 26 (1), 43–58.

Stokes, R.A., 1989. Calculation file for soil water model—concept and theoretical basis of soil water model for the southwest of Western Australia. Unpublished Report, Water Authority of WA, Water Resources Directorate.

Tamai, N., 1992a. Discharge prediction for flow in a compound channel: a new approach to overbank flow. Part 1. Evaluation of floodplain resistance. Civ. Engng Trans., Inst. Engrs Aust. CE34 (4), 285–294.

Tamai, N., 1992b. Discharge prediction for flow in a compound channel: a new approach to overbank flow. Part 2. Discharge prediction based on a depth-averaged flow equation. Civ. Engng Trans., Inst. Engrs Aust. CE34 (4), 295–302.

Woltemade, C.J., Potter, K.W., 1994. A watershed modeling analysis of fluvial geomorphologic influences on flood peak attenuation. Water Resour. Res. 30, 1933–1942.

Wong, T.H.F., 1989. Nonlinearity in catchment flood response. Civ. Engng Trans., Inst. Engrs Aust. CE31 (1), 30–37.

Wong, T.H.F., Laurenson, E.M., 1983. Wave speed–discharge relations in natural channels. Water Resour. Res. 19, 701–706.

Wood, E.F., Sivapalan, M., Beven, K., 1990. Similarity and scale in catchment storm response. Rev. Geophy. 28, 1–18.

Wormleaton, P.R., Merrett, D.J., 1990. An improved method of calculation for steady uniform flow in prismatic main channel/flood plain sections. J. Hydraul. Res. 28 (2), 157–174.